ZERO-POWER ACOUSTIC WAKE-UP RECEIVER BASED ON DMUT TRANSMITTER, PMUTS ARRAYS RECEIVERS AND MEMS SWITCHES FOR INTRABODY LINKS

Flavius Pop[*1], *Bernard Herrera*[1], *William Zhu*[1], *Meruyert Assylbekova*[1], *Cristian Cassella*[1], *Nicol McGruer*[1], *Matteo Rinaldi*[1]
[1]SMART Center, ECE Department, Northeastern University, Boston, USA

ABSTRACT

This paper demonstrates, for the first time, a zero-power acoustic wake-up receiver for intrabody links, allowing Implanted Medical Devices (IMDs) to minimize the IDLE power consumption. This architecture is based on Directly Modulated Ultrasonic Transducers (dMUT) made of Lead Zirconate Titanate (PZT) as transmitter (TX), a Piezoelectric Micro Machined Ultrasonic Transducer (pMUT) array as receiver (RX), and a Micro Electro-Mechanical System (MEMS) switch. The role of the dMUTs and the pMUT array is to establish an acoustic link sensitive to signals as low as $50mV_{pp}$ peak-peak at a distance of $10cm$. This low signal triggers the switch which will turn on the IMDs from an IDLE-state to a full power mode.

KEYWORDS

Implanted Medical Devices (IMD), Directly Modulated Ultrasonic Transducer (dMUT), Piezoelectric Micro Machined Ultrasonic Transducer (pMUT), Micro Electro-Mechanical (MEMS) Switch, Acoustic Wake-up Receiver, Intrabody Communication, Internet of Medical Things (IoMT)

INTRODUCTION

In recent years, the number of devices connected to the "Internet of Things (IoT)", such as smart-phones, home appliances, wearable, sensors etc., has exponentially increased. The common requirement to all these devices are: miniaturization, wireless communication, low power consumption and low cost. As part of the IoT there are also the health-care devices, in particular the Implanted Medical Devices (IMD) [1], forming the "Internet of Medical Things IoMT". The IMDs in a human body can be connected together to form a Wireless Body Area Network (WBAN) and use the living tissue as transmission channel. The WBAN can collect vital signs from the patient and transmit them to a health care access point where a physician will monitor them. Similarly, the WBAN can receive external commands and send internal stimulus to the body to treat a certain illness (e.g. insulin pump acting on the sensing of glucose level in the blood).

The IMDs can be divided in three main categories, depending on their function. The first one are the diagnostic IMDs, in charge of sensing vital signs of a patient. Some examples are the glucose sensor [2] and oximeter for pulse sensing [3]. The seconds are the therapeutic devices that directly treat an ailment by applying a stimulus to the body. Some examples are the pacemaker [4] (the very first IMD in 1950s) and brain stimulators [5]. The third are the assisting IMDs are meant for the improving of anatomical and physiological functions. Some examples are the cochlear implants to improve the hearing [6] and bionic vision implants [7] (bionic eye). The implantation depth can very between a few millimeters (sub-cutaneous or trans-cutaneous implantation) to several centimeters (the pacemaker is implanted at $12cm$), thus is important the choice of the communication technology.

One option is to use Radio Frequency (RF) antennas that uses radio wave propagation in the body [8]. This method suffers from strong attenuation of the waves in the tissue, thus limiting the implantation depth. Another method is to modulated the magnetic filed generated by an implanted inductive coil and then couple it to an external coil [9]. While allowing higher data rate and more power transfer, this method also suffers from attenuation of the magnetic field in the living tissue and it is affected by external interference on the same operational bandwidth. An alternative is to modulate the electric field, either through capacitive coupling [10] or galvanic coupling [11]. The first one if affected by external noise and the second is hard to model.

Recently, new emerging method are proposed, such as optical and ultrasound communication. The optical approach makes use of Vertical Cavity Surface Emitting Lasers (VCSEL) to modulate the Infrared (IR) waves as carrier signal. This operates in the GHz to THz range, thus limiting the implantation depth to a few millimeter due to IR absorption [12]. The second method, instead, uses acoustic wave as carrier signal. The advantages is that those are mechanical waves and they propagate with less attenuation in the human tissue, giving it's elastic nature [13]. The commercial available acoustic transducers are bulky and not bio-compatible, such as the Lead Zirconate Titanate (PZT) based [14], therefore they cannot be implanted. Instead, these can still be used externally as a high acoustic power source.

As a bio-compatible and miniaturized alternative, Micromachined Ultrasonic Transducers (MUTs) are proposed. Their main structure consists of a membrane that is designed to resonate in a flexural mode allowing the generation of acoustic waves. The MUTs can be distinguished in two categories based on their actuation mechanism. The first ones are the capacitive MUTs (cMUTs) [15], which are actuated through an electric field. Since the cMUTs require a high DC bias and a high AC actuation voltage, their electronic circuits are more complex and packaging is more challenging (to avoid burning the human tissue with high DC levels). The second type are the piezoelectric MUTs (pMUTs) [16]. These take advantage of the intrinsic property of piezoelectric materials to mechanically deform when small AC voltages are applied, allowing the suspended membrane to vibrate and generate acoustic waves, without the need of a DC bias . The most common micromachined piezoelectric material is the Aluminum Nitride (AlN) [17], given its high coupling coefficient between the mechanical and electrical domain (k_t^2), its low mechanical losses (high quality factor Q), and its bio-compatibility [18]. Recent research on pMUTs based on Scandium doped AlN (ScAlN) [19] and micromachined PZT [20], has shown promising improvements in the k_t^2, which allows the generation of higher acoustic pressures, which can increase the implantation depth. In this work the pMUTs are AlN-based.

The pMUTs have been explored for a broad range of applications including intrabody communication [13, 21, 22, 23]. MEMS switches have already been employed in RF zero-power wake-up receivers [24]. Instead, dMUTs only recently have been proposed for directly modulating the signal of pMUT arrays and enable high data rates in acoustic communication links [25]. In this work, we present, for the first time, a wake-up receiver based on dMUTs. The system is capable of triggering intrabody wireless nodes with record low received acoustic power, thus enabling unprecedented reduction of their IDLE-power consumption.

WAKE-UP SYSTEM DESCRIPTION

The acoustic wake-up receiver's architecture consists of a dMUT system driving a PZT acoustic transducer (TX external device to the body) and a pMUT array (RX implantable in the body). As a first demonstration, both devices are submerged in a De-Ionized (DI) water tank, at a distance of $10cm$, to establish and emulate an intrabody acoustic link. The RX array is then connected to a MEMS switch, which is placed in a vacuum chamber in order to minimize the squeezed dumping effect and maximize the Q [24].

The resonance frequency of both PZT and pMUTs is $700kHz$ ($f_{PZT} = f_{pMUTs}$). Instead, the resonance frequency of the MEMS switch ranges from 130kHz, when its gate is unbiased ($V_G = 0V_{DC}$), to 110kHz when the gate is biased ($V_G = 6V_{DC}$). The frequency is down shifting because of the the spring softening effect [24]. The dMUT system allows to mix, on top of the acoustic link, a low frequency component. This signal introduced by the direct modulation system is designed to match the resonance frequency of the MEMS switch ($f_{MOD} = f_{SW}$).

Given the high-quality factor of the switch ($Q = 9000$), only the low frequency component of the acoustic signal will be filtered by the switch and consequently triggered by it once a threshold voltage level is reached. The dMUT [25] consists of a Bipolar Junction Transistor (BJT) driven as a switch. This will allow to switch the connection between an LC filter (that is DC biased) to the PZT TX. This transition will generate high AC voltages due to the sudden change in capacitance seen by the transducer. The main idea is to release all the charge accumulated in the LC filter in a very shot period of time, thus generating high AC voltages. This feature allows to maximize the output pressure generated by the transducer, which ultimately translates into a higher received signal and into a higher sensitivity achieved by the presented wake-up receiver architecture. The transmitted signal is then received at $10cm$ by a pMUT array and the pressure is converted into AC voltage due to the piezoelectric effect.

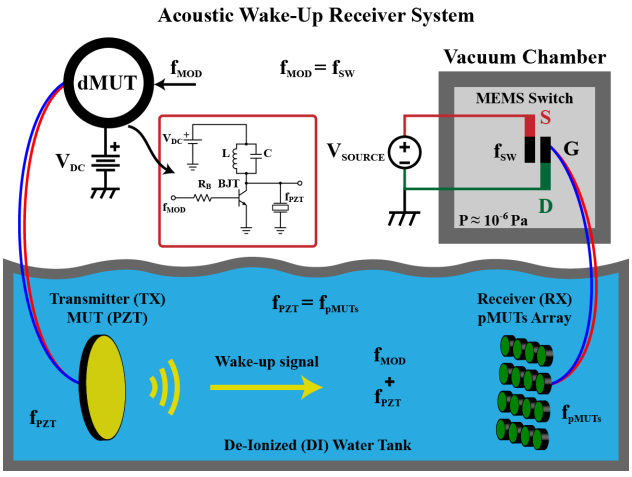

Figure 1: *Acoustic wake-up receiver system. A dMUT system [25] is used to modulate, on top of a PZT transducer (TX) acoustic signal (f_{PZT}), a low carrier frequency signal (f_{MOD}). The acoustic link is formed in a DI water tank (to emulate an intrabody medium) and received by a pMUT array (RX) which is designed at the same frequency of the PZT (f_{pMUT}). At this point the array is connected to a MEMS switch which is placed in a vacuum chamber (to minimize the squeezed dumping effect [24]). Furthermore, thanks to the dMUT system, the signal on top of the TX is further amplified through the charging effect of an LC thank (see inset). Overall, the acoustic signal at the pMUTs is able to wake-up the MEMS switch and turn-on an IMD from an IDLE state.*

MEMS DEVICES CHARACTERIZATION

The pMUTs were laid out in arrays of 45 columns and 50 rows per chip, for a total dimension of $8 \times 8mm^2$. Each individual pMUT consist of a circular membrane of radius $a = 46\mu m$ and the following stack layers: $0.8\mu m$ of Silicone Di-Oxide (SiO_2), $0.1\mu m$ of Platinum (Pt), $0.75\mu m$ of Aluminum Nitride (AlN) and $0.15\mu m$ of Gold (Au). Based on this design parameters, the theoretical resonance frequency is around $f_{res} = 700kHz$ in DI water. Fig. 2a. shows an optical image of the fabricated pMUT array. Fig. 2b. reports on the Digital Holographic Microscope (DHM) measurement of the displacements of individual pMUTs, while Fig. 2c. shows a 3D rendering of the displacement of a sub-set of pMUTs in the array.

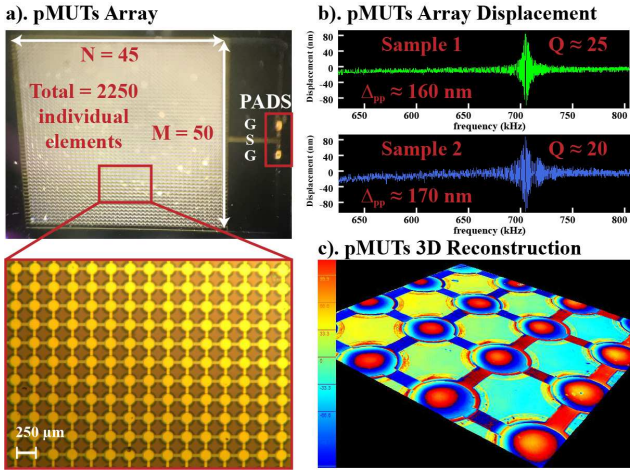

Figure 2: *a). Fabricated pMUT array as a receiver in the wake-up acoustic system. The array consists of $N = 45$ columns and $M = 50$ rows for a total of 2250 single elements (inset zoom-in). b). Digital Holographic Microscopes (DHM) measurement of the displacement of two different membranes of the pMUTs. The total displacement ranges from $160nm$ to $170nm$ peak-peak (for $10V$ AC input signal) with a measured quality factor $Q = 20 - 25$ underwater. The resonance frequency is around $700kHz$ as designed. c). 3D reconstruction a 3x3 grid of pMUTs from the fabricated array.*

In Fig. 3 are shown the top-view (a) and lateral-view (b) Scanning Electron Microscope (SEM) images of the MEMS switch. Fig. 3 reports on the measured displacement of the switch while driving it with $10,000$ burst cycles of $100mV_{pp}$ peak-peak. The measured quality factor is $Q = 9000$. Further details on the design and fabrication of the switch are reported in [24].

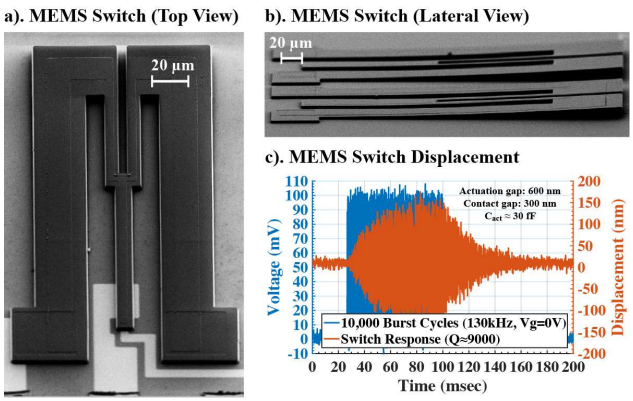

Figure 3: *Scanning Electron Microscope (SEM) image of the fabricated MEMS switch: a). top view and b). lateral view. c). Laser Doppler Vibrometer (LDV) measurement of the switch while being excited with 10,000 pulsed burst cycles.*

EXPERIMENTAL RESULTS

The wake-up system was tested in a DI water tank, where the acoustic transducers were submerged, and the MEMS switch placed in a vacuum chamber. The maximum reached sensitivity of the RX pMUT array is $50mV_{pp}$ peak-peak, at a distance of $10cm$ from the TX array. For this configuration, the switch's gate is biased at $V_G = 6V_{DC}$ (just below the pull-in voltage) and the source and drain are connected to a multi-meter while applying a $V_{SD} = 200mV_{AC}$. When the acoustic link is formed between the TX PZT and RX pMUT array, the switch if fully closed and a current of $1\mu A$ can be read from source and drain. This demonstrates the capability of using pMUTs as wake-up receiver elements, with zero-power consumption, allowing very-low IDLE-power for IMDs.

In Fig. 4 is shown the output wave generated by the dMUT system (blue curve) on top of the PZT transducers. This output consists of high AC voltages releases (up to $85Vpp$) and spaced by the modulation frequency, which is set at the input of the dMUT. This wave will then acoustically propagate in the water at the speed of $1500m/s$. The two main loss mechanisms are the geometric spread (the energy is conserved but is spread on spheres of larger and larger radius as it propagates forward) and an exponential medium absorption (0.1 dB/m in water). At $10cm$ in water, the received signal by the fabricated pMUT arrays is shown in Fig. 4 (orange curve). This received signal shows an intensity of around $50mV_{pp}$ peak-peak. The signal will contain the transmitted pulse by the PZT and a modulated component at around $100kHz$, which will trigger the MEMS switch through the received signal by the pMUT array.

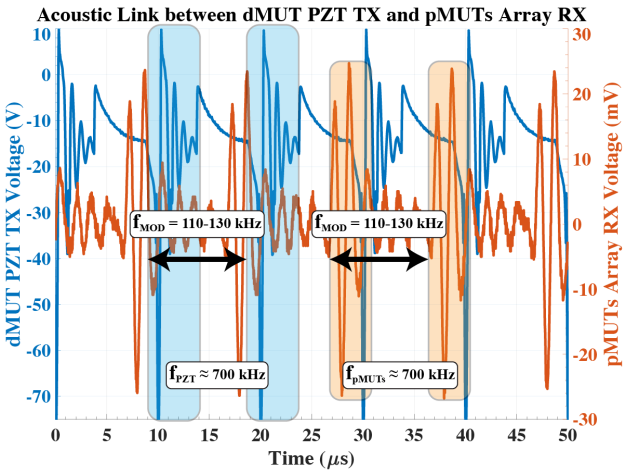

Figure 4: *Experimental data of the signal generated by the dMUT on top of the PZT (TX) and the received signal through the acoustic link on the pMUT array (RX).*

In Fig. 5 is shown the activation of the MEMS switch based on the received signal on the pMUT array. In order to make the switch sensitive to $50mV$, a DC bias is applied. This static voltage level will physically decrease the MEMS switch gap between the metal contacts. The gap is minimized when the V_{DC} is close to the pull-in voltage. By minimizing the MEMS switch gap, less AC voltage is required to turn on the switch. The switch was tuned on by the AC voltage when using $6V$ of DC bias. The current in the OFF-state is in the pA range (noise level). Instead, in the ON-state, the measured current is in the order of μA when applying a voltage of $V_{SD} = 200mV$ between the source and the drain of the switch. Given the high quality factor (Q) of the switch, this will be highly selective to the modulation frequency.

It was noticed that if the switch is kept on the ON-state for long periods ($> 10ms$), the switch will maintain the state even when the acoustic signal is turned off. This happened because the metal contacts where stuck together due to the stiction force. In future implementations, the MEMS switch will be designed to minimize the stiction force when the electrodes are in contact. An alternative is to design another terminal on the opposite side of the switch, which will restore the OFF-state after the switch goes in contact.

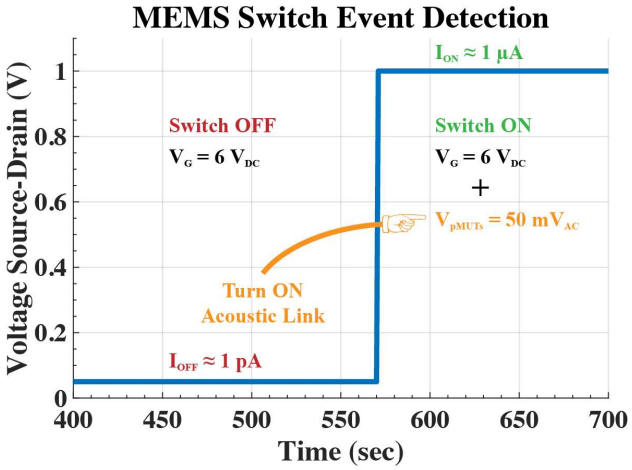

Figure 5: *MEMS switch event detection measurement. The MEMS switch is biased close to the pull-in voltage in order to minimize the voltage needed to actuate it. Then, the acoustic link is turned activated and, with only $V_{pMUTs} = 50mV_{AC}$, the switch was turned on. The current measurement goes from $I_{off} = 1pA$ (noise level) to $I_{on} = 1\mu A$. This demonstrates the wake-up capability of the system.*

Since the wake-up system is acoustically triggered, it is important to compute the Sound Pressure Level (SPL) by which the MEMS switch is activated and brought to the ON-state from the IDLE-state. Each individual pMUT will contribute to build up the received voltage based on the average power available at $10cm$ from the transmitter (assuming that all the array elements are working). Moreover, since the triggering signal is out of resonance, this will not be enhanced by the Q of the pMUTs. The average received pressure by a pMUT and its displacement are given by: $P_{av} = 2\pi f_{res} d_{av} \rho c/N$ and $d_{av} \approx a^2/De_{31f} z_P V$, where $\rho = 1000kg/m^3$ is the medium density (water in this case), $c = 1500m/s$ is the propagation speed of acoustic waves in water, N is the total number of pMUTs, D is the plate rigidity of the pMUT, $e_{31f} = -1.02C/m^2$ is the piezoelectric coefficient, z_P is the distance between the piezoelectric layer and the neutral axis and V is the received voltage. Base on this formulas, the average pressure is estimated to be $P_{av} = 175mPa$, which corresponds to $SPL = 20log_{10}(P_{av}/P_{ref}) = 105dB$, where $P_{ref} = 1\mu Pa$.

CONCLUSION

This work demonstrates for the first time an acoustic wake-up receiver for intrabody networks. The communication link is based on a dMUT system that drives a PZT transducer as transmitter (external) and pMUT arrays (implantable in the body) as receiver. The dMUT allows to transmit a low frequency signal along with the main carrier frequency of the acoustic transducers. The array is then connected to a MEMS switch that is highly selective to the low modulation frequency ($Q = 9000$). The switch is triggered by a signal as low as $50mVpp$, thus corresponding to an $SPL = 105dB$. This demonstrates the high sensitivity of the system to very low acoustic signal, thus enabling zero-power acoustic wake-up receivers for IMDs.

ACKNOWLEDGMENTS

This work was supported by the NSF programs MRI-SEANet (NSF Number 1726512) and NeTS-Small (NSF Number 1618731). Authors would also like to thank the stuff of the George J. Kostas Nanoscale Technology and Manufacturing Research Center for helping with the microfabrication.

REFERENCES

[1] A. Kiourti and K. S. Nikita, "A review of in-body biotelemetry devices: Implantables, ingestibles, and injectables," *IEEE Transactions on Biomedical Engineering*, vol. 64, no. 7, pp. 1422–1430, 2017.

[2] Y. Yu, T. Nguyen, P. Tathireddy, D. J. Young, and S. Roundy, "Wireless hydrogel-based glucose sensor for future implantable applications," in *2016 IEEE SENSORS*, pp. 1–3, IEEE, 2016.

[3] B. K. Rivera, S. K. Naidu, K. Subramanian, M. Joseph, H. Hou, N. Khan, H. M. Swartz, and P. Kuppusamy, "Real-time, in vivo determination of dynamic changes in lung and heart tissue oxygenation using epr oximetry," in *Oxygen Transport to Tissue XXXVI*, pp. 81–86, Springer, 2014.

[4] F. V. Tjong and V. Y. Reddy, "Permanent leadless cardiac pacemaker therapy: a comprehensive review," *Circulation*, vol. 135, no. 15, pp. 1458–1470, 2017.

[5] S. Little, A. Pogosyan, S. Neal, B. Zavala, L. Zrinzo, M. Hariz, T. Foltynie, P. Limousin, K. Ashkan, J. FitzGerald, *et al.*, "Adaptive deep brain stimulation in advanced parkinson disease," *Annals of neurology*, vol. 74, no. 3, pp. 449–457, 2013.

[6] M. Yip, R. Jin, H. H. Nakajima, K. M. Stankovic, and A. P. Chandrakasan, "A fully-implantable cochlear implant soc with piezoelectric middle-ear sensor and arbitrary waveform neural stimulation," *IEEE journal of solid-state circuits*, vol. 50, no. 1, pp. 214–229, 2015.

[7] A. J. Lowery, J. V. Rosenfeld, M. G. Rosa, E. Brunton, R. Rajan, C. Mann, M. Armstrong, A. Mohan, H. Josh, L. Kleeman, *et al.*, "Monash vision group's gennaris cortical implant for vision restoration," in *Artificial Vision*, pp. 215–225, Springer, 2017.

[8] B. Kibret, A. K. Teshome, and D. T. Lai, "Characterizing the human body as a monopole antenna," *IEEE Transactions on Antennas and Propagation*, vol. 63, no. 10, pp. 4384–4392, 2015.

[9] T. Kagami, H. Matsutani, M. Koibuchi, Y. Take, T. Kuroda, and H. Amano, "Efficient 3-d bus architectures for inductive-coupling thruchip interfaces," *IEEE Transactions on Very Large Scale Integration (VLSI) Systems*, vol. 24, no. 2, pp. 493–506, 2016.

[10] T. G. Zimmerman, "Personal area networks: near-field intrabody communication," *IBM systems Journal*, vol. 35, no. 3.4, pp. 609–617, 1996.

[11] T. Handa, S. Shoji, S. Ike, S. Takeda, and T. Sekiguchi, "A very low-power consumption wireless ecg monitoring system using body as a signal transmission medium," in *Proceedings of International Solid State Sensors and Actuators Conference (Transducers' 97)*, vol. 2, pp. 1003–1006, IEEE, 1997.

[12] M. Faria, L. N. Alves, and P. S. de Brito André, "Transdermal optical communications," in *Visible Light Communications*, pp. 331–358, CRC Press, 2017.

[13] G. E. Santagati and T. Melodia, "Experimental evaluation of impulsive ultrasonic intra-body communications for implantable biomedical devices," *IEEE Transactions on Mobile Computing*, vol. 16, no. 2, pp. 367–380, 2017.

[14] E. Moulin, J. Assaad, C. Delebarre, H. Kaczmarek, and D. Balageas, "Piezoelectric transducer embedded in a composite plate: application to lamb wave generation," *Journal of Applied Physics*, vol. 82, no. 5, pp. 2049–2055, 1997.

[15] H. Nan, K. C. Boyle, N. Apte, M. S. Aliroteh, A. Bhuyan, A. Nikoozadeh, B. T. Khuri-Yakub, and A. Arbabian, "Non-contact thermoacoustic detection of embedded targets using airborne-capacitive micromachined ultrasonic transducers," *Applied Physics Letters*, vol. 106, no. 8, p. 084101, 2015.

[16] A. Guedes, S. Shelton, R. Przybyla, I. Izyumin, B. Boser, and D. Horsley, "Aluminum nitride pmut based on a flexurally-suspended membrane," in *2011 16th International Solid-State Sensors, Actuators and Microsystems Conference*, pp. 2062–2065, IEEE, 2011.

[17] M.-A. Dubois and P. Muralt, "Properties of aluminum nitride thin films for piezoelectric transducers and microwave filter applications," *Applied Physics Letters*, vol. 74, no. 20, pp. 3032–3034, 1999.

[18] N. G. Berg, T. Paskova, and A. Ivanisevic, "Tuning the biocompatibility of aluminum nitride," *Materials Letters*, vol. 189, pp. 1–4, 2017.

[19] Y. Kusano, G.-L. Luo, D. Horsley, I. taru Ishii, and A. Teshigahara, "36% scandium-doped aluminum nitride piezoelectric micromachined ultrasonic transducers," in *2018 IEEE International Ultrasonics Symposium (IUS)*, pp. 1–4, IEEE, 2018.

[20] Y. Kusano, Q. Wang, G.-L. Luo, Y. Lu, R. Q. Rudy, R. G. Polcawich, and D. A. Horsley, "Effects of dc bias tuning on air-coupled pzt piezoelectric micromachined ultrasonic transducers," *Journal of Microelectromechanical Systems*, vol. 27, no. 2, pp. 296–304, 2018.

[21] Z. Guan, G. E. Santagati, and T. Melodia, "Ultrasonic intra-body networking: Interference modeling, stochastic channel access and rate control," in *2015 IEEE Conference on Computer Communications (INFOCOM)*, pp. 2425–2433, IEEE, 2015.

[22] F. V. Pop, B. Herrera, C. Cassella, G. Chen, E. Demirors, R. Guida, T. Melodia, and M. Rinaldi, "Novel pmut-based acoustic duplexer for underwater and intrabody communication," in *2018 IEEE International Ultrasonics Symposium (IUS)*, pp. 1–4, IEEE, 2018.

[23] F. Pop, B. Herrera, C. Cassella, and M. Rinaldi, "pmut-based real-time (rt) acoustic discovery architecture (ada) for intrabody networks (in)," in *Joint Frequency Control Symposium and European Frequency and Time Forum, 2019 IEEE International*, p. tbd, IEEE, 2019.

[24] W. Z. Zhu, T. Wu, G. Chen, C. Cassella, M. Assylbekova, M. Rinaldi, and N. McGruer, "Design and fabrication of an electrostatic aln rf mems switch for near-zero power rf wake-up receivers," *IEEE Sensors Journal*, vol. 18, no. 24, pp. 9902–9909, 2018.

[25] F. Pop, B. Herrera, C. Cassella, and M. Rinaldi, "Direct modulation piezoelectric micro-machined ultrasonic transducer system (dmut)," in *Micro-Electro Mechanical Systems (MEMS), 2019 IEEE International*, p. tbd, IEEE, 2019.

CONTACT

*Flavius Pop - flavius.pop@ieee.org - LinkedIn